Guiding Waves Along an Infinitesimal Line between Impedance Surfaces

Dia'aaldin J. Bisharat and Daniel F. Sievenpiper

Phys. Rev. Lett. **119**, 106802 — Published 8 September 2017

DOI: 10.1103/PhysRevLett.119.106802

Guiding waves along an infinitesimal line between impedance surfaces

Dia'aaldin J. Bisharat[1,2*] and Daniel F. Sievenpiper[2*]

[1]*Department of Electronic Engineering, City University of Hong Kong, Kowloon, Hong Kong, China*
[2]*Electrical and Computer Engineering Department, University of California, San Diego, California, 92093, USA*
**dbisharat2-c@my.cityu.edu.hk; dsievenpiper@eng.ucsd.edu*

We present a new electromagnetic mode that forms at the interface between two planar surfaces laid side by side in free space, effectively guiding energy along an infinitesimal, one-dimensional line. It is shown that this mode occurs when the boundaries have complementary surface impedances, and it is possible to control the mode confinement by altering their values correspondingly. The mode exhibits singular field enhancement, broad bandwidth, direction-dependent polarization, and robustness to certain defects. As a proof-of-concept, experimental results in the microwave regime are provided using patterned conducting sheets. Our proposed effective-medium-based approach is general, however, thus allowing for potential implementation up to optical frequencies. Our system is promising for applications including integrated photonics, sensing, switching, chiral quantum coupling, and reconfigurable waveguides.

Having a peak field bound to the interface of two media makes surface-waves (SWs) [1] attractive for energy transmission with simple implementation for sensing and communication applications [2,3]. Exploiting plasmon polaritons' nature [4], SWs can exhibit strong light confinement which is useful for realizing subwavelength guiding structures, hence high-density integration of optical circuits and lower waveguide bending loss. Variations such as V-shaped grooves [5] and wedges [6], albeit with more complexity, reduce SWs to one dimension (1D) despite the absence of an enclosing structure, thus enabling greater guiding control. Similarly, guided modes at the edge of photonic crystals (PCs), within shared bulk and surface bandgaps, have been proposed [7]. In addition, edge plasmons have been observed in graphene ribbons [8].

Recently, there has been a special attention to structures with interface modes exhibiting robust directional propagation. Notably, this includes photonic topological insulators based on symmetry-protected topological (SPT) phases [9,10,11,12]. In these systems, where time-reversal (TR) symmetry is not broken [13,14,15,16], crystalline or intrinsic symmetries of the wave fields and differing topology of bulk bands give rise to wavevector-locked states at the interface [12]. Analogously, opposite single-negative bulk materials [17] support bound states that exhibit a similar though limited robustness [18,19,20]. In addition, trivial structures such as nanofibers and glide-plane PC waveguides [21], where light is tightly confined with evanescent wave on their interface, can exhibit direction-dependent polarizations [22].

In this work, we introduce a new 1D mode, analogous yet different from SWs, that is confined to the interface-line between two planes. The line-wave (LW) possesses robust wavevector-locked states, broad bandwidth, strong -ideally singular- field enhancement and tunable mode confinement. We analyze how LW can arise due to complementary surface-impedances and demonstrate experimentally its feasibility using periodic surfaces with suitable effective-medium properties. Furthermore, we examine the characteristics of our system at different conditions and suggest possible applications. Our work opens a new door for planar, compact and efficient routing and concentration of electromagnetic energy, and for unconventional devices.

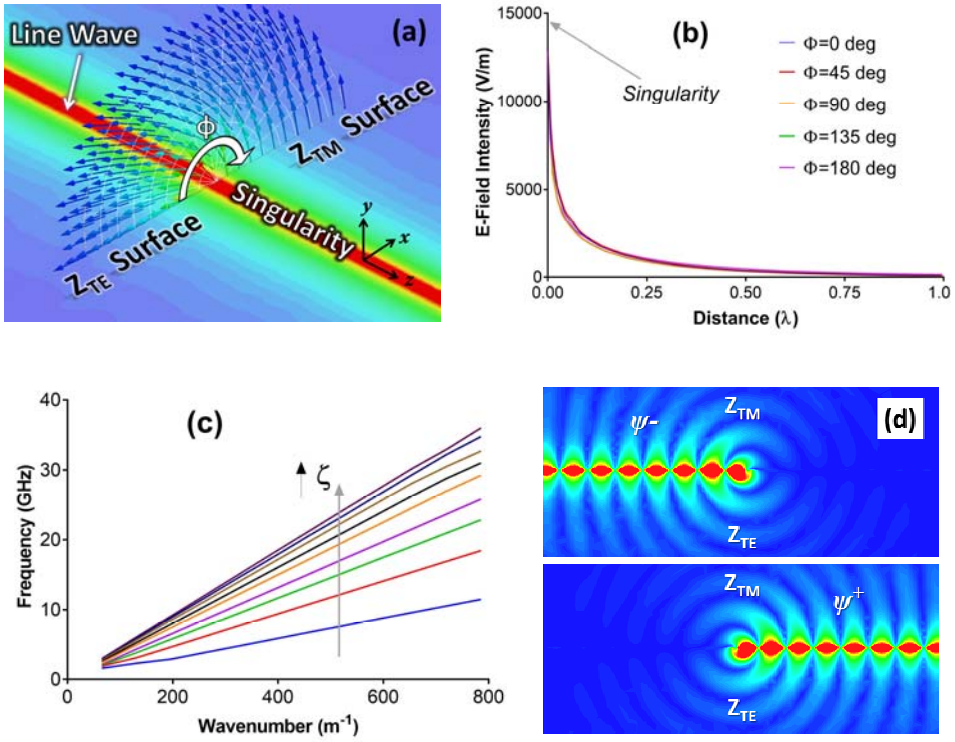

FIG. 1 (color online). Simulated field characteristics of line-wave. (a) Magnitude distribution and vector plot of the *E*-field above the interfaced TE and TM surfaces (linear scale), (b) decay profile of the *E*-field at different directions about the interface-line, (c) dispersion of the line mode at different values of complementary impedances, and (d) pseudo-spin states excited by electric and magnetic Hertzian dipoles along y-axis in-phase (above) or out-of-phase (below).

SW modes can be guided on planar structures with subwavelength periodic inclusions, known as metasurfaces [23,24], whose response to impinging waves and their guiding properties can be conveniently characterized by surface-impedance [25,26]. This methodology has been extensively used for variety of applications including electromagnetic guiding, absorption, radiation, scattering alteration, cloaking, and self-focusing [27,28,29,30,31,32]. Consider a field

with an exponential decay $e^{-\alpha y}$ away from the surface and a propagation function $e^{-j\beta z}$, such that $\alpha^2 = \beta^2 - k^2$, where k is the wavenumber in free space. The surface-impedances for transverse-magnetic (TM) and transverse-electric (TE) polarized waves are [33]:

$$Z_{TM} = j\eta_0 \frac{\alpha}{k} \quad , \quad Z_{TE} = -j\eta_0 \frac{k}{\alpha} \tag{1}$$

where η_0 is the intrinsic impedance of free space. Meanwhile, the refractive index n seen by the SW is $n = c / v_p = \beta / k$, where c is the speed of light in free space and v_p is the phase velocity of the wave along the surface. Therefore, the relationship between the surface-impedance and the refractive index is [34]:

$$Z_{TM} = \eta_0 \sqrt{1 - n^2} \quad , \quad Z_{TE} = \eta_0 / \sqrt{1 - n^2} \tag{2}$$

Accordingly, for TM- and TE-polarized SWs propagating at equal phase velocities, we can define a new parameter ζ that relates the two respective surface-impedances as:

$$j\frac{Z_{TE}}{\eta_0} = j\frac{\eta_0}{Z_{TM}} = \zeta \tag{3}$$

First, consider the case where ζ is infinite, so that the TM- (TE-) surface becomes a perfect electric (magnetic) conductor, PEC (PMC). Obviously, the PEC (PMC) boundary forces the tangential electric (magnetic) field to vanish, thus allowing only the TM (TE) SW mode to survive. When interfacing the two surface types, as shown in Fig. 1a, a new localized mode, which is a product of interference between TM and TE modes, appears at the interface. Consequently, the associated *E*-field vectors point in the transverse direction adjacent to the Z_{TE} surface and vary gradually toward the normal direction as we trace a path at constant distance away from the interface towards the Z_{TM} surface. Hence, using cylindrical coordinates, the waveform of the mode is deduced as [35] (see Supplementary Material [36]):

$$E_z = E_0 K_{\frac{1}{2}}(\alpha\rho)\ \mathrm{Sin}\left(\frac{\phi}{2}\right)e^{-j\beta z} \quad , \quad H_z = \frac{E_0}{\eta_0} K_{\frac{1}{2}}(\alpha\rho)\ \mathrm{Cos}\left(\frac{\phi}{2}\right)e^{-j\beta z} \tag{4}$$

where *K* is the modified Bessel function of the second kind, and $\alpha^2 = k^2 - \beta^2$, with $\beta \geq k$.

The waveform is verified with full wave simulation in ANSYS HFSS software, which clearly shows the singular nature of field intensity at the interface, as depicted in Fig. 1b. Here, for a given ζ value, the field intensity decays away from the interface at different ϕ angles at the same rate. Note that although the field is infinite at the interface-line, the field everywhere has a finite integral; thus the power carried by LW is finite. Just as SWs on good conductors are only loosely bound to the surface, this is also the case for LWs, which have $\beta = k$ for the limit of a PEC-PMC interface. A more tightly bound mode is readily attainable by adopting a finite ζ

value, hence $\beta > k$, as shown in Fig. 1c. Note that regardless of ζ value, the field remains infinite at the line in the absence of loss [36].

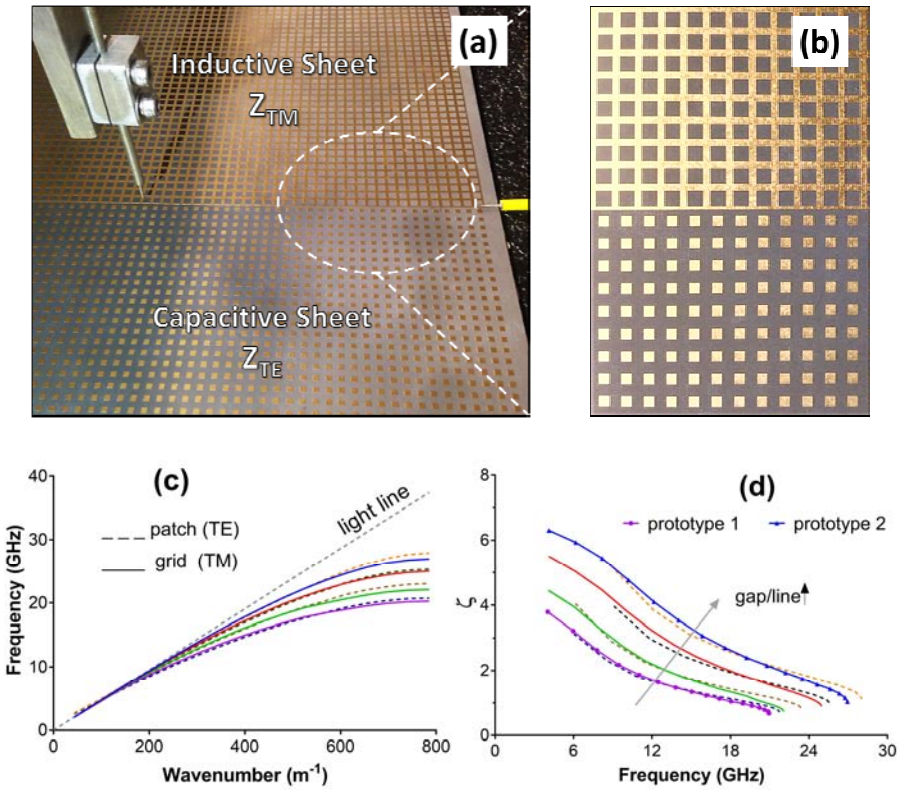

FIG. 2 (color online). Measurement setup and characteristics of the fabricated FSS sheets. (a) A probe antenna (right) oriented along the interface-line is used as the excitation source while another probe (left) oriented vertically at a 1 □ 2mm distance above to the surface is used to scan the relative intensity of the normal *E*-field component, (b) zoom-in of the complementary FSS sheets fabricated on a printed-circuit-board (PCB) on Rogers 5880 (ε_r = 2.2, $\delta_t = 0.001$) substrate with a 0.8mm thickness, (c) dispersion characteristics of TM and TE FSS cells of different sizes, and (d) ζ values versus frequency for different sizes of FSS cells. Prototypes 1 and 2 both have unit cell period of 4mm. Prototype 1 (2) has grid-line width of 0.2mm (1.2mm) and gap width of 0.8mm (2.2mm) between patches.

To realize the LW, two surfaces whose impedances take the form in equation (3) are required, i.e. an inductive (capacitive) surface to support a TM (TE). These criteria can be fulfilled by simple frequency-selective surfaces (FSS) such as these shown in Fig. 2b. Here, the conducting grid (patches) exhibits a dominant inductive (capacitive) response at frequencies where the FSS cell is subwavelength. Fig. 2c shows that the respective SW modes of the complementary surface have dispersion curves (phase velocities) that overlap over a wide bandwidth as desired [38]. Fig. 2d shows the associated ζ values, including for the two fabricated prototypes, at different frequencies.

Fig. 3a, which maps the relative intensity of the normal *E*-field component measured at a fixed distance above the impedance surfaces, shows successful excitation and transmission of LW along the interface for a distance of several wavelengths. As shown in Fig. 3b, the normal *E*-field component is evident on both sides of the interface, as expected, albeit with slightly larger amplitude on the TM side (positive *x*-axis). Moreover, due to lower ζ values, prototype 1 exhibits greater field concentration than prototype 2, as expected. The simulated and measured results across the interface at roughly 1□2mm above the surface are in good agreement. On the other hand, the simulated field intensity at the center of the interface shows higher enhancement level [36] with an effective mode width of less than $\lambda_0/15$.

The measured operation range, which spans roughly two octaves of bandwidth, could be extended by adopting other artificial surfaces with lesser dispersion and broader overlap between the complementary dispersion curves. In addition, the fields at the singularity are limited in physical implementations by the thickness of the surface, dissipation losses, and periodicity of the FSS structures [36]. Thus, at higher frequencies up to the optical domain, it is more suitable to use 2D materials such as graphene at the terahertz regime, which features highly-confined long-lifetime plasmons [39]. Importantly, graphene can be modeled as an impedance sheet and support TM and TE SWs depending on its doping level [40]; hence allowing straightforward implementation and tunabilty thanks to the universality of the proposed effective surface-impedance approach.

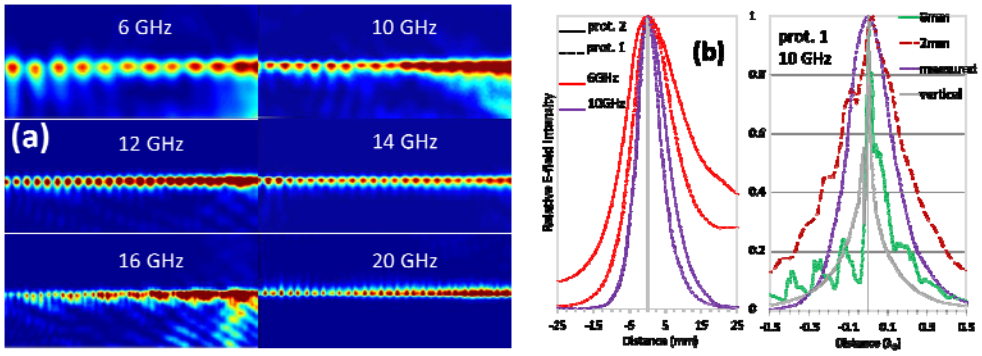

FIG. 3 (color online). Measured results of the line-wave. (a) *E*-field magnitude distribution at different frequencies on top of prototype 1 (left) and prototype 2 (right), and (b) normalized decay curves of the normal *E*-field component along the transverse direction to the interface-line (linear scale) at 1-2mm above the two prototypes (left) and comparison with simulated results at 2mm and 0mm above the surface as well as through origin along the normal (vertical) direction to the surface (right).

Another important aspect is that the LW exhibits wavevector-locked states. Joined PEC ($\varepsilon=-\infty,\mu=1$) and PMC ($\varepsilon=1,\mu=-\infty$) boundaries may preserve -an otherwise broken-electromagnetic duality by forming mirror images about the *yz* plane satisfying the $\varepsilon(x)=\mu(-x)$ inversion-symmetry [41,42]. Note that a single PEC-PMC interface is sufficient to partially

bound energy due to ε-negative and μ-negative materials possessing different topological orders when considering a fixed wave polarization [18,19,20]. As the new decoupled interface modes form a hybrid of magnetic and electric modes with a specific phase relationship, they possess conserved pseudo-spin values [43,36]. Also, since the pseudo-spin configuration is uniquely defined by the direction of the propagation wavevector (β), the interface constitutes a spin-filtered channel [10,41**Error! Bookmark not defined.**]. This makes our system somewhat reminiscent of TR-invariant SPT states formed between two claddings of opposite bianisotropy [12], where intrinsic symmetries of the fields and differing topology of bulk bands give rise to counter propagating pseudo-spin states, ψ^+ and ψ^- [36].

The approach above can be generalized to interfacing inductive-capacitive surfaces with identical ζ value. Notably, this solves the issue of the weak cross coupling between TM and TE modes in the PEC-PMC case, which otherwise necessities using a closed waveguide configuration for practical applications. The paradigm of effective surface-impedance has been exploited in relation with band geometric (Zak) phases to explain the appearance of interface states in 1D and 2D systems of PCs [44,45]. In comparison, our system is free of the bandwidth limitation associated with bandgaps in PCs, and supports direction-dependent polarizations as evident from the full-wave simulation shown in Fig. 1d. Note that although the spin-momentum locking property is universal in evanescent waves [22], it is more prominent in the case of LW due to the strict confinement in the transverse plane to the wavevector leading to 1D propagation only.

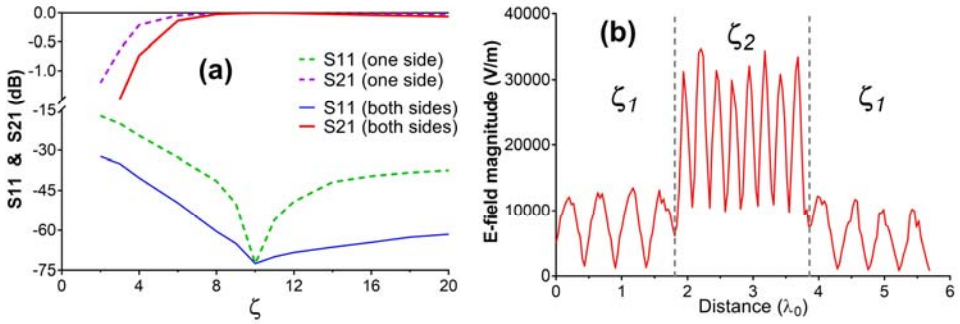

FIG. 4 (color online). Influence of a finite discontinuity in surface-impedance on the line-wave. (a) Transmission and reflection coefficients of the mode due to a defect ($\zeta \neq 10$) at one or both sides of the interface over a distance of $0.6\lambda_0$, and (b) snapshot of field magnitude depicting an increased enhancement and a shorter wavelength over a finite distance due to change in surface-impedances across the interface.

The spin-momentum locking feature enforced by the boundary-inversion symmetry endows our line guide with robustness against reflection from certain structural defects. To qualify this symmetry-protection, we introduce a discrete discontinuity in surface-impedance over a finite distance along the interface [36]. As shown in Fig. 4a, for a large impedance variation

($6 \le \zeta \le 20$) in either one or both impedance surfaces, reflection coefficient (S_{11}) lower than -30dB and isolation (S_{21}) of about -0.1dB are achieved. This is expected given that such defect does not violate spin-degeneracy or cause reversal of boundary conditions. The larger reflection in case of one-sided impedance discontinuity is because of the degraded boundary symmetry, which leads to mismatch in phase velocity across the interface. This result, though does not show complete immunity to backscattering, somewhat emulates topological protection [36].

This symmetry-protection allows for variations in the field enhancement and propagation constant of the LW at arbitrary sections of the waveguide, as shown in Fig. 4b. For example, this enables the design of compact and lossless delay lines without the need for any bends. However, switching the impedance surfaces' orientation across the interface forbids the LW propagation [36]. This is useful for building network devices, with simple implementation, such as magic T-structure as shown in Fig. 5a. Here, the LW fed at port 1 is guided to ports 2 and 4 with no energy coupling to port 3 as desired.

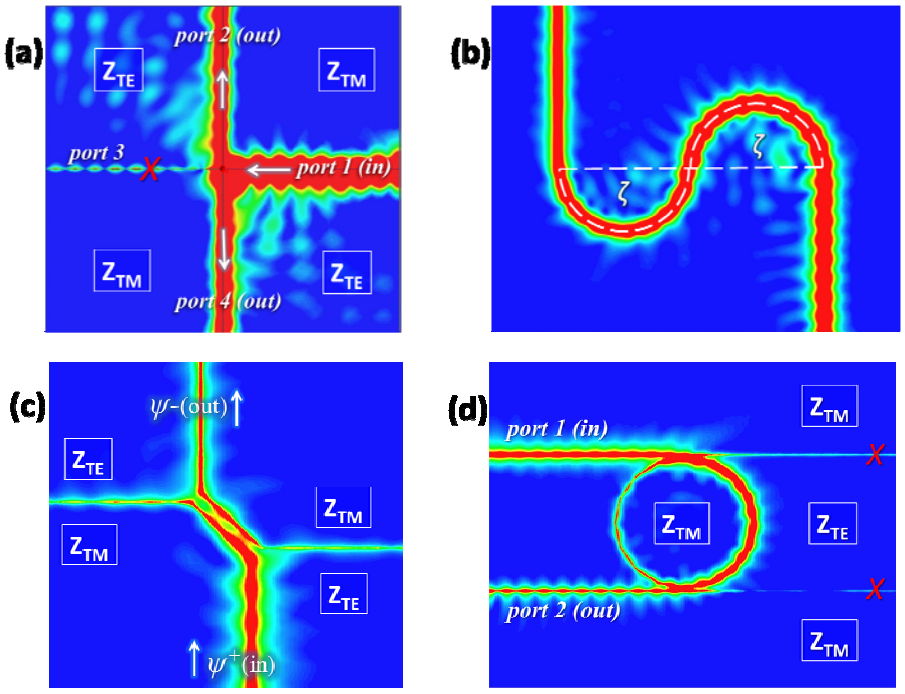

FIG. 5 (color online). Full-wave simulations for potential applications of the line-wave. (a) Wave transmission in four-port network (magic-T) of a junction due to surface-impedance reversal, (b) wave transport along a curved interface-line with a proper change in TM and TE surface-impedances, (c) coupler structure showing excitation of a reversed pseudo-spin mode, and (d) an implementation of a ring-resonator showing frequency selection.

One the other hand, guiding LW along a bent path causes scattering similarly to conventional SWs along a curved surface [36]. Although the LW mode must be localized near the interface, energy can couple to the SW modes that are supported at the same frequency (i.e. no surface

bandgap). As shown in Fig. b, this leakage can be prevented by adjusting the relative ζ values across the interface so that the mismatch between the respective phase velocities is amended. Alternatively, this feature can be exploited, for instance, to form a coupler device that could transfer energy between eigenfields of the opposite pseudospin-polarizations, as shown in Fig. 5c. Also, this allows the formation of a ring resonator device, as shown in Fig. 5d, for filtering applications.

The above findings make LW appealing for energy confinement, transport and integrated photonics applications, as 1D object being the smallest waveguide possible. Also, due to its planar configuration, strong mode confinement [46] and pseudospin-polarization [**Error! Bookmark not defined.**], LW is attractive for light-matter interaction and chiral quantum processes [21,36]). Moreover, the significant field enhancement and the available air channel at the interface-line can potentially offer simple implementation for micro-plasma and vacuum-based electronic devices [47]. Furthermore, the adopted effective-medium approach allows for forming LWs with reconfigurable pathways [48,40]. The associated tuning capability and the field singularity may also pave the way to nonlinear photonic structures for switching and modulation applications [49].

This work has been supported in part by AFOSR grant FA9550-16-1-0093.

References:

[1] J. A. Jr. Polo, T. G. Mackay, and A. Lakhtakia, *Electromagnetic Surface Waves: A Modern Perspective, 1st ed.* (Elsevier Inc., London, 2013)
[2] J. Homola, *Surface Plasmon Resonance Based Sensors* (Springer, 2006)
[3] M. Dragoman and D. Dragoman, Prog. Quantum Electron. 32, 1–41 (2008)
[4] A. V. Zayats, I. I. Smolyaninov, and A. A. Maradudin, Phys. Rep. 408, 131–314 (2005)
[5] S. I. Bozhevolnyi, V. S. Volkov, E. Devaux, J. Y. Laluet, and T. W. Ebbesen, Nature 440, 508–511 (2006)
[6] E. Moreno, S. G. Rodrigo, S. I Bozhevolnyi, L. Martín-Moreno, and F. J. García-Vidal, Phys. Rev. Lett. 100, 023901 (2008)
[7] L. Lu, J. D. Joannopoulos, and M. Soljačić, Phys. Rev. Lett. 108, 243901 (2012)
[8] A. Y. Nikitin, F. Guinea, F. J. Garcia-Vidal, and L. Martín-Moreno, Phys. Rev. B 84, 161407(R) (2011)
[9] A. B. Khanikaev et al., Nature Mater. 12, 233–239 (2013)
[10] T. Ma, A. B. Khanikaev, S. H. Mousavi, and G. Shvets, Phys. Rev. Lett. 114, 127401 (2015)
[11] L.-H. Wu and X. Hu, Phys. Rev. Lett. 114, 223901 (2015)
[12] Slobozhanyuk, A. et al. Nat. Photonics 11, 130-136 (2017)
[13] L. Lu, J. D. Joannopoulos, and M. Soljačić, Nature Photon. 8, 821–829 (2014)
[14] M. Hafezi, E. A. Demler, M. D. Lukin, and J. M. Taylor, Nat. Phys.7, 907–912 (2011)
[15] W. Gao et al., Phys. Rev. Lett. 114, 037402 (2015)
[16] M. C. Rechtsman et al., Nature 496, 196–200 (2013)
[17] A. Alù and N. Engheta, IEEE. T. Antenn. Propag. 51(10), 2558–2571 (2003)
[18] W. Tan, Y. Sun, H. Chen, and S.-Q. Shen, Sci. Rep. 4, 3842 (2014)
[19] X. Shi, C. Xue, H. Jiang, and H. Chen, Opt. Exp. 24(16), 18580 (2016)

[20] M. G. Silveirinha, Phys. Rev. B 93, 075110 (2016)
[21] P. Lodahl et al. Nature 541, 473-480 (2017)
[22] T. Van Mechelen and Z. Jacob, Optica 3, 118–126 (2016)
[23] F. J. Garcia-Vidal, L. Martín-Moreno, and J. B. Pendry, J. Opt. A: Pure Appl. Opt. 7, S97 (2005)
[24] S. Maci, G. Minatti, M. Casaletti, and M. Bosiljevac, IEEE Antennas Wireless Propag. Lett., vol. 10, 1499–1502, (2011)
[25] B. H. Fong, J. S. Colburn, J. J. Ottusch, J. L. Visher, and D. F. Sievenpiper, IEEE Trans. Antenn. Propag., 58(10), 3212-3221 (2010)
[26] H. J. Bilow, IEEE Trans. Antenn. Propag. 51(10), 2788-2792 (2003)
[27] F. Elek, B. B. Tierney, and A. Grbic, IEEE Trans. Antenn. Propag. 63(9), 3956–3962 (2015)
[28] R. Quarfoth and D. Sievenpiper, IEEE Trans. Antenn. Propag., 63(10), 4593–4599 (2015)
[29] A. M. Patel and A. Grbic, IEEE Trans. Antenn. Propag. 59(6), 2087–2096 (2011)
[30] H. Wakatsuchi, S. Kim, J. J. Rushton, and D. F. Sievenpiper, Phys. Rev. Lett. 111, 245501 (2013)
[31] P.-Y. Chen and A. Alù, Phys. Rev. B 84, 205110 (2011)
[32] Z. Lou, X. Chen, J. Long, R. Quarfoth, and D. Sievenpiper, Appl. Phys. Lett. 106, 211102 (2015)
[33] Ramo, Whinnery, Van Duzer, *Fields and Waves in Communication Electronics, 2nd ed.* (John Wiley and Sons, New York, 1984)
[34] D. F. Sievenpiper, *High-Impedance Electromagnetic Surfaces*. PhD thesis (UCLA, 1999)
[35] Jian-Ming Jin, *Theory and Computation of Electromagnetic Fields, 1st ed.* (Wiley, New Jersey, 2010)
[36] See Supplemental Material at [url], which includes Ref. [37], for additional details, discussions and results.
[37] J. D. Kraus and R. J. Marhefka, *Antenna: For All Applications 3rd Ed*. (Mc Graw Hill, New York, 2002)
[38] M. Lei, S. Xiao, J. Long, and D. F. Sievenpiper, IEEE Trans. Antenn. Propag. 64(9), 3811–3819 (2016)
[39] F. J. García de Abajo, ACS Photonics 1, 135–152 (2014)
[40] A. Vakil and N. Engheta, Science 332, 1291–1294 (2011)
[41] W.-J. Chen, Z.-Q. Zhang, J.-W. Dong, and C. T. Chan, Nat. Commun. 6,8183 (2015)
[42] M. G. Silveirinha, Phys. Rev. B 95, 035153 (2017)
[43] L. Marrucci, Nat. Physics 11, 9–10 (2015)
[44] M. Xiao, Z. Q. Zhang, and C. T. Chan, Phys. Rev. X 4, 021017 (2014)
[45] M. Xiao, X. Huang, A. Fang, and C. T. Chan, Phys. Rev. B 93, 125118 (2016)
[46] A. F. Koenderink, A. Alù, and Polman, Science 348, 516–521 (2015)
[47] E. Forati, T. J. Dill, A. R. Tao, and D. Sievenpiper, Nat. Commun. 7, 13399 (2016)
[48] X. Cheng et al., Nature Mater. 15, 542–548 (2016)
[49] M. Kauranen and A. V. Zayats, Nature Photonics 6, 737–748 (2012)